

# Mid-infrared trace gas detection using continuous-wave difference frequency generation in periodically poled RbTiOAsO<sub>4</sub>

W. Chen<sup>1,\*</sup>, G. Mouret<sup>1</sup>, D. Boucher<sup>1</sup>, F.K. Tittel<sup>2</sup>

<sup>1</sup>MREID, Université du Littoral, 145 Av. Maurice Schumann, 59140 Dunkerque, France

<sup>2</sup>Rice Quantum Institute, MS 366, Rice University, 6100 Main St., Houston, TX 77005, USA

Received: 23 October 2000/Revised version: 22 January 2001/Published online: 27 April 2001 – © Springer-Verlag 2001

**Abstract.** A tunable mid-infrared continuous-wave (cw) spectroscopic source in the 3.4–4.5  $\mu\text{m}$  region is reported, based on difference frequency generation (DFG) in a quasi-phase-matched periodically poled RbTiOAsO<sub>4</sub> (PPRTA) crystal, DFG power levels of 10  $\mu\text{W}$  were generated at approximately 4  $\mu\text{m}$  in a 20-mm long PPRTA crystal by mixing two cw single-frequency Ti:Al<sub>2</sub>O<sub>3</sub> lasers operating near 713 nm and 871 nm, respectively, using a laser pump power of 300 mW. A quasi-phase-matched infrared wavelength-tuning bandwidth (FWHM) of  $\sim 12 \text{ cm}^{-1}$  and a temperature tuning rate of  $1.02 \text{ cm}^{-1}/^\circ\text{C}$  were achieved. Experimental details regarding the feasibility of trace gas detection based on absorption spectroscopy of CO<sub>2</sub> in ambient air using this DFG radiation source are also described.

**PACS:** 42.72.Ai; 42.65.Ky

In recent years there have been rapid developments in quasi-phase-matching (QPM) bulk materials for efficient optical frequency conversion applications. In a ferroelectric optical material, QPM is usually implemented by periodic reversal of ferroelectric domains. To date, periodically poled LiNbO<sub>3</sub> (PPLN) [1], KTiOPO<sub>4</sub> (PPKTP) [2, 3], KTiOAsO<sub>4</sub> (PPKTA) [4], and RbTiOAsO<sub>4</sub> (PPRTA) [5–7] have been either commercially available or have been experimentally investigated for use in optical parametric devices. Quasi-phase-matched PPRTA crystal offers several distinct advantages compared to other periodically poled ferroelectric optical materials for non-linear interactions. The optical transparency range for PPRTA extends to about 5.8  $\mu\text{m}$  at long wavelengths (at the zero transmittance level) [8, 9], as compared to 5.5  $\mu\text{m}$  for PPLN, 4.5  $\mu\text{m}$  for PPKTP and 5.3  $\mu\text{m}$  for PPKTA [9]. Unlike PPLN, which suffers from absorption in the 4–5  $\mu\text{m}$  region, PPRTA has the added benefit of significantly reduced absorption within this region. The non-linear optical figure of merit, defined as  $d_{\text{eff}}^2/n^3$  (where  $d_{\text{eff}}$  and  $n$

are the effective non-linear optical coefficient and refractive index respectively), of PPRTA is  $21.5 \text{ pm}^2/\text{V}^2$ , which is comparable to that of PPLN ( $27 \text{ pm}^2/\text{V}^2$ ). In addition, PPRTA possesses a high damage threshold of  $> 400 \text{ MW}/\text{cm}^2$  (at 1064 nm for pulses of 10–20 ns duration), which is approximately five times higher than that for PPLN. Furthermore, its coercive field for electric poling is approximately ten times lower than that of PPLN, which should facilitate periodic poling of several mm-thick samples. The last two characteristics are advantageous for non-linear frequency conversion when using high-power pump sources. PPRTA is thus an attractive alternative to PPLN for non-linear optical frequency conversion-based coherent light generation in the region of 3–5  $\mu\text{m}$ . In addition, PPRTA crystal has a significantly higher resistance to photorefractive damage than PPLN, which permits stable operation of the crystal at room temperature.

Until now, PPRTA crystals have been employed mostly in cw optical parametric oscillators (OPO) [5], pulsed OPO [6, 10, 11] or pulsed DFG [7]. Recently, Fradkin et al. reported cw mid-infrared generation (3.25–3.7  $\mu\text{m}$ ) by quasi-phase-matched DFG in a multi-grating periodically poled RTA crystal, which allowed the characterization of optical and non-linear properties of the crystal [12]. In fact, a tunable mid-infrared light source based on DFG in PPRTA is important for applications in high-resolution spectroscopy and ultra sensitive trace gas sensing. Furthermore, QPM data obtained from cw DFG measurements permit further characterization of the non-linear optical properties of PPRTA in the infrared.

## 1 Experimental procedure

The DFG architecture used in this work is shown in Fig. 1. Two cw single-frequency Ti:Sapphire (Ti:Al<sub>2</sub>O<sub>3</sub>) lasers were used as convenient versatile laboratory DFG pump sources. The laser beams, polarized parallel to the  $z$ -axis of the PPRTA crystal, were collinearly focused onto the crystal using a 35-cm-focal length lens, which produced an identical beam waist for each laser of about 80  $\mu\text{m}$  by using a quasi-achromatic Gaussian optical system [13]. The PPRTA

\*Corresponding author.

(Fax: +33-3/2865-8244, E-mail: chen@univ-littoral.fr)

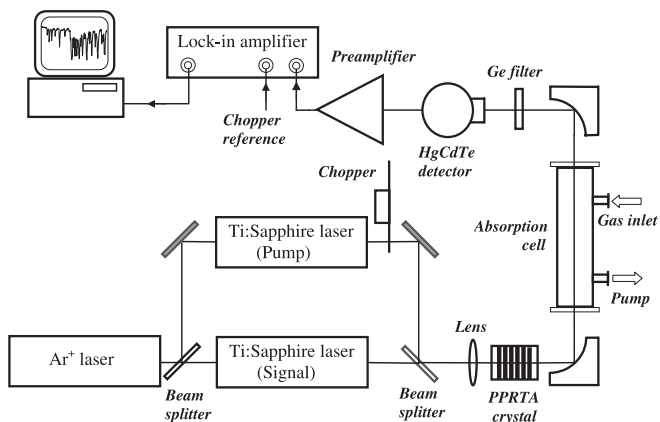


**Fig. 1.** Experimental arrangement for generating mid-infrared radiation by difference frequency mixing of two single frequency titanium-sapphire lasers in a quasi-phase-matching periodically poled RbTiOAsO<sub>4</sub> crystal

crystal was 1 mm thick, with a 20-mm-interaction length and a quasi-phase-matched period of 24.1  $\mu\text{m}$  (Crystal Associates Inc.). The end-faces were optically polished and uncoated. Figure 2 shows a microphotograph of the etched grating domain pattern (100 $\times$ ), taken with a polarization optical microscope (Leitz DM RXP). The infrared emission was collimated with a parabolic mirror, and directed to a single-pass or multi-pass gas absorption cell. The infrared detector was a liquid nitrogen-cooled HgCdTe photoconductive detector with a  $1 \times 1 \text{ mm}^2$  active area. A 1-mm-thick uncoated germanium (Ge) filter was employed as a long-wavelength pass filter to block unwanted pump and signal laser beams. The output signal from the detector was amplified by a low-noise preamplifier and fed to a lock-in amplifier.

Infrared radiation was generated with broad wavelength tunability in the 3.4–4.5  $\mu\text{m}$  region using Ti:Al<sub>2</sub>O<sub>3</sub> lasers, tunable from 710 to 720 nm, and 847 to 915 nm, respectively. A quasi-phase-matched wavelength-tuning bandwidth (FWHM) of approximately 12  $\text{cm}^{-1}$  was observed when the signal laser wavelength was fixed at 845 nm and the pump wavelength was scanned near 710 nm. Experimental QPM laser wavelengths for infrared generation from 3.4 to 4.5  $\mu\text{m}$  are depicted as dots in Fig. 3. The predicted values, based on the Sellmeier equation, are also plotted for comparison. The offset in the maximum QPM conversion wavelength from that calculated theoretically [7]

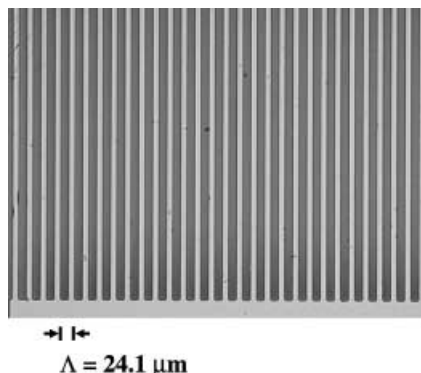


**Fig. 2.** Side view microphotograph (100 $\times$ ) of the etched PPRTA grating domain pattern

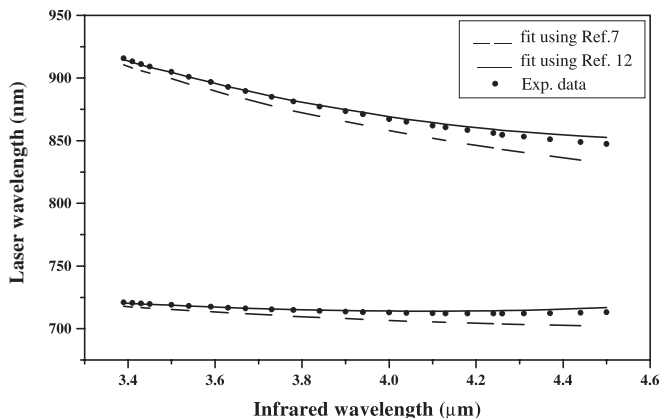


**Fig. 3.** Quasi-phase-matching characteristics of the PPRTA crystal at room temperature. The generated infrared wavelength as a function of the mixed laser wavelengths is shown. The *dashed* and *solid* curves represent calculated values based on the Sellmeier equation given in [7] and [12], respectively, and *dots* indicate experimental data

(dashed lines) was about  $-220 \text{ cm}^{-1}$  at 4.5  $\mu\text{m}$ . This apparent discrepancy is mainly due to the fact that the Sellmeier coefficients given in [7] were derived from refractive index measurements for wavelengths ranging from 403 nm to 3.6  $\mu\text{m}$ , using the minimum-deviation technique. An improved dispersion equation was reported recently in [12] (represented by solid lines in Fig. 3) by fitting the cw QPM-DFG data in the 1.53–3.48  $\mu\text{m}$  range and the measurements of Fenimore et al. [7] in the 0.8–1.3  $\mu\text{m}$  range. The maximum offset has been reduced to  $\sim 73 \text{ cm}^{-1}$  at 4.5  $\mu\text{m}$ .

Infrared light powers of 10  $\mu\text{W}$  were produced at 4  $\mu\text{m}$  by mixing the output from two Ti:Al<sub>2</sub>O<sub>3</sub> lasers operating near 871 nm (100 mW) and 713 nm (200 mW), respectively, which corresponds to a power intensity of 1.5  $\text{kW}/\text{cm}^2$ . The experimental focusing function  $h(\xi, \mu)$  [14, 15] was determined to be about 0.18, with  $\xi = 0.23$  and  $\mu = 0.81$ , where  $\xi$  is the ratio of the interaction length to confocal parameter, and  $\mu$  is the ratio of the signal and pump wave vectors. After correction for Fresnel losses from the optical components in the set-up, these pumping conditions yielded a power conversion efficiency of  $\sim 0.5 \text{ mW}/\text{W}^2 \text{ cm}^{-1}$  at room temperature. An effective non-linear coefficient of  $d_{\text{eff}} = 11.2 \text{ pm}/\text{V}$  was thus derived from the experimental DFG efficiency at 4  $\mu\text{m}$ . The corresponding non-linear coefficient  $d_{33}$  was determined to be 17.5  $\text{pm}/\text{V}$ , which is slightly higher than the value of  $d_{33} = 15.8 \text{ pm}/\text{V}$  reported in [16]. The conversion coefficient can be further improved by a factor of approximately two by using more tightly focused beams (with  $\xi = 1.3$ , the focusing parameter  $h$  attains its maximum value of 0.3 under the focusing conditions in the experiment).

Pump power induced temperature effects were also investigated and found to be about  $5 \text{ }^\circ\text{C}/\text{W}$ , which is similar to those for AgGaS<sub>2</sub> as used in our work reported previously [17]. The slope of the temperature-dependent wavelength tuning was found to be  $-1.02 \text{ cm}^{-1}/^\circ\text{C}$ , which is comparable to that for PPLN [18] and about two times higher than that for PPKTP [19]. The infrared wavelength tuning of the DFG power is shown in Fig. 4 at 25.2  $^\circ\text{C}$  and 51.5  $^\circ\text{C}$ , respectively. In this experiment, the signal wavelength was fixed at  $\sim 871 \text{ nm}$ , and the pump laser was scanned to track

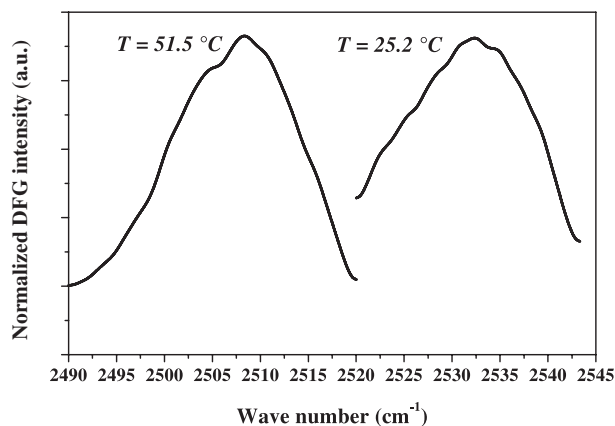


**Fig. 4.** Infrared wavelength tuning characteristics of DFG power output at 25.2 °C and 51.5 °C, respectively

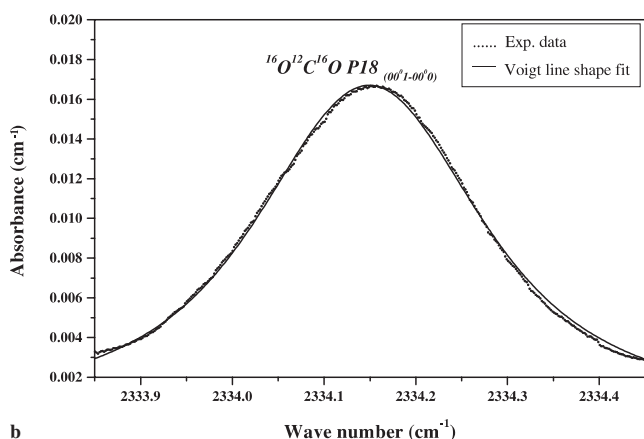
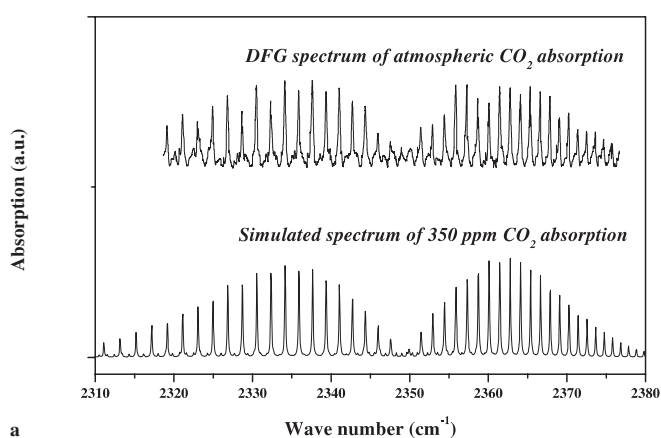


**Fig. 5. a** Absorption spectrum of the  $\nu_3$  band of carbon dioxide in ambient air measured at room temperature and atmospheric pressure, using a mid-IR spectroscopic source based on DFG in PPRTA crystal (*top*), compared with the Hitran database simulation of 350 ppm  $\text{CO}_2$  absorption spectrum (*bottom*). The experimental and simulated spectra have the same linear vertical scale (absorbance per cm, as shown in Fig. 5b), and are displaced for visual clarity. **b** High-resolution absorption spectrum of the  $\nu_3$ -P(18) line (*dots*). The *solid line* is a Voigt curve to the absorption line. Spectroscopic measurement yielded a  $\text{CO}_2$  concentration of  $\sim 350$  ppm present in ambient laboratory air

the phase-matching condition. A large degree of temperature tuning is desirable for widely tunable optical parametric devices.

Measurements of the absorption spectrum of the  $\nu_3$  band of carbon dioxide ( $\text{CO}_2$ ) in ambient air were carried out using the QPM-PPRTA-based infrared source. The spectrum shown in Fig. 5a (top line) was measured ( $\sim 10 \text{ cm}^{-1}/\text{scan}$ ) at room temperature and atmospheric pressure with an open optical path of 22.5 cm between the crystal and the infrared detector. Figure 5a (bottom line) shows a Hitran database [20] simulation of 350 ppm  $\text{CO}_2$  absorption in the atmosphere. The experimental and simulated spectra have the same linear vertical scale (absorbance per cm, as shown in Fig. 5b), and are displaced for visual clarity. Figure 5b is a high-resolution  $\text{CO}_2$  absorption spectrum of the observed  $\nu_3$ -P(18) line (*dots*). The *solid line* is a Voigt curve fitted to the absorption line. A  $\text{CO}_2$  concentration of  $\sim 350$  ppm in the laboratory's ambient air was deduced from the spectroscopic measurement.

## 2 Summary

In summary, a cw coherent infrared source with broad and rapid tuning characteristics in the 3.4–4.5  $\mu\text{m}$  spectral region has been obtained by difference-frequency generation in a 20-mm-long periodically poled  $\text{RbTiOAsO}_4$  crystal. A DFG power conversion efficiency of up to approximately  $0.5 \text{ mW}/\text{W}^2 \text{ cm}^{-1}$  was achieved at 4  $\mu\text{m}$ . The wavelength and temperature tuning characteristics of the mid-infrared DFG-based spectroscopic source were determined. The large damage threshold combined with broadband temperature tuning, as well as the high thermal conductivity, makes PPRTA an attractive material when using high-power cw fiber amplifiers and diode-pumped solid-state lasers as convenient DFG pump sources. With increased pump powers, DFG powers in the several-mW range should be attainable. Broad tunability over the 3.0–5.0  $\mu\text{m}$  range can be obtained by QPM-PPRTA-based DFG using different grating periods. This wavelength region is of particular interest for atmospheric monitoring of greenhouse gas such as  $\text{CO}_2$ ,  $\text{CH}_4$ ,  $\text{H}_2\text{S}$ ,  $\text{H}_2\text{CO}$  and environmental sensing of various toxic hydrocarbon gases, such as BTEX (Benzene–Toluene–Ethylbenzene–Xylene), as shown in Fig. 6. The 3–5  $\mu\text{m}$  range is also of particular interest for high-resolution spectroscopy of pure carbon clus-

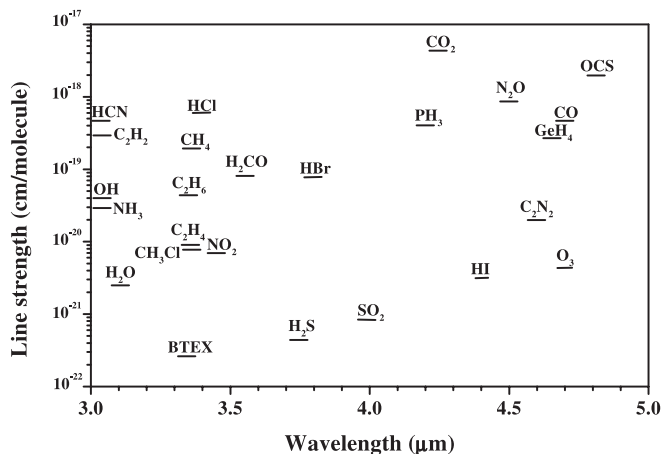


**Fig. 6.** Spectroscopic survey of line strengths of important atmospheric trace gases and toxic pollutants in the 3–5  $\mu\text{m}$  infrared region

ters, which has wide applicability from dust grain formation in the interstellar medium to soot formation in combustion systems [21].

*Acknowledgements.* The Laboratoire de Physicochimie de l'Atmosphère participates in the Centre d'Études et de Recherches Lasers et Applications (CERLA) supported by the Ministère Chargé de la Recherche, the Région Nord-Pas de Calais and the Fonds Européen de Développement Économique des Régions. We gratefully thank Dr. J.J. Zondy of BNM-LPTF (Paris) for his helpful discussion and comments, and Dr. F. Roussel for the PPRTA grating domain pattern picture.

## References

1. L.E. Myers, W.R. Bosenberg: IEEE J. Quantum Electron. **QE-33**, 1663 (1997)
2. K. Fradkin, A. Arie, A. Skliar, G. Rosenman: Appl. Phys. Lett. **74**, 914 (1999)
3. A. Garashi, A. Arie, A. Skliar, G. Rosenman: Opt. Lett. **23**, 1739 (1998)
4. K. Fradkin-Kashi, A. Arie, P. Urenski, G. Rosenman: Opt. Lett. **25**, 743 (2000)
5. T.J. Edwards, G.A. Turnbull, M.H. Dunn, M. Ebrahimzadeh, H. Karlsson, G. Arvidsson, F. Laurell: Opt. Lett. **23**, 837 (1998)
6. H. Karlsson, M. Olson, G. Arvidsson, F. Laurell, U. Bäder, A. Borstutzky, R. Wallenstein, S. Wickström, M. Gustafsson: Opt. Lett. **24**, 330 (1999)
7. D.L. Fenimore, K.L. Schepler, D. Zelmon, S. Kuck, U.B. Ramabadran, P. Von Richter, D. Small: J. Opt. Soc. Am. B **13**, 1935 (1996)
8. C. Tu, R. Katiyar, V. Schmidt, R. Guo, A. Bhalla: Phys. Rev. B **59**, 251 (1999)
9. V.G. Dmitriev, G.G. Gurzadyan, D.N. Nikogosyan: *Handbook of Non-linear Optical Crystals*, Springer Series in Optical Science No. 64 (1997)
10. G.T. Kennedy, D.T. Reid, A. Miller, M. Ebrahimzadeh, H. Karlsson, G. Arvidsson, F. Laurell: Opt. Lett. **23**, 503 (1998)
11. P. Loza-Alvarez, D.T. Reid, M. Ebrahimzadeh, W. Sibbett, H. Karlsson, P. Henriksson, G. Arvidsson, F. Laurell: Appl. Phys. B **68**, 177 (1999)
12. K. Fradkin-Kashi, A. Arie, P. Urenski, G. Rosenman: Appl. Phys. B **71**, 251 (2000)
13. W. Chen, J. Burie, D. Boucher: Spectrochim. Acta A **55**, 2057 (1999)
14. T. Chu, M. Broyer: J. Phys. (France) **46**, 523 (1985)
15. J.J. Zondy: Opt. Commun. **149**, 181 (1998)
16. L.K. Cheng, L.T. Cheng, J. Galperin, P.A. Morris Hotsenpiller, J.D. Bierlein: J. Crystal Growth **137**, 107 (1994)
17. W. Chen, J. Burie, D. Boucher: Rev. Sci. Instrum. **67**, 3411 (1996)
18. D.H. Jundt: Opt. Lett. **22**, 1553 (1997)
19. G.M. Gibson, G.A. Turnbull, M. Ebrahimzadeh, M.H. Dunn, H. Karlsson, G. Arvidsson, F. Laurell: Appl. Phys. B **67**, 675 (1998)
20. L.S. Rothman, C.P. Rinsland, A. Goldman, S.T. Massie, D.P. Edwards, J.M. Flaud, A. Perrin, C. Camy-Peyret, V. Dana, J.Y. Mandin, J. Schroeder, A. McCann, R.R. Gamache, R.B. Wattson, K. Yoshino, K.V. Chance, K.W. Jucks, L.R. Brown, V. Nemtchinov, P. Varanasi: J. Quant. Spectrosc. Radiat. Transfer **60**, 665 (1998)
21. T.F. Giesen, A. Van Orden, H.J. Hwang, R.S. Fellers, R.A. Provençal, R.J. Saykally: Science **265**, 756 (1994)